

ACCELERATED PUBLICATION

Solar cell efficiency tables (version 51)

Martin A. Green¹  | Yoshihiro Hishikawa²  | Ewan D. Dunlop³ | Dean H. Levi⁴ |
 Jochen Hohl-Ebinger⁵ | Anita W.Y. Ho-Baillie¹ 

¹Australian Centre for Advanced Photovoltaics, University of New South Wales, Sydney, 2052, Australia

²Research Center for Photovoltaics (RCPV), National Institute of Advanced Industrial Science and Technology (AIST), Central 2, Umezono 1-1-1, Tsukuba, Ibaraki, 305-8568, Japan

³Directorate C—Energy, Transport and Climate, European Commission—Joint Research Centre, Via E. Fermi 2749, IT-21027 Ispra, VA, Italy

⁴National Renewable Energy Laboratory, 15013 Denver West Parkway, Golden, CO 80401, USA

⁵Department of Characterisation and Simulation/Callab Cells, Fraunhofer-Institute for Solar Energy Systems, Heidenhofstraße 2, D-79110 Freiburg, Germany

Correspondence

Martin A. Green, School of Photovoltaic and Renewable Energy Engineering, University of New South Wales, Sydney, 2052, Australia.
 Email: m.green@unsw.edu.au

Funding information

U.S. Department of Energy, Grant/Award Number: DE-AC36-08-GO28308

Abstract

Consolidated tables showing an extensive listing of the highest independently confirmed efficiencies for solar cells and modules are presented. Guidelines for inclusion of results into these tables are outlined and new entries since July 2017 are reviewed, together with progress over the last 25 years. Appendices are included documenting area definitions and also listing recognised test centres.

KEYWORDS

energy conversion efficiency, photovoltaic efficiency, solar cell efficiency

1 | INTRODUCTION

Since January 1993, *Progress in Photovoltaics* has published 6 monthly listings of the highest confirmed efficiencies for a range of photovoltaic cell and module technologies.^{1,2} By providing guidelines for inclusion of results into these tables, this not only provides an authoritative summary of the current state-of-the-art but also encourages researchers to seek independent confirmation of results and to report results on a standardised basis. In version 33 of these tables,² results were updated to the new internationally accepted reference spectrum (International Electrotechnical Commission IEC 60904-3, Ed. 2, 2008).

The most important criterion for inclusion of results into the tables is that they must have been independently measured by a recognised test centre listed in Appendix A (note 2 recent additions). A distinction is made between 3 different eligible definitions of cell area: total area, aperture area, and designated illumination area, as defined in Appendix B. “Active area” efficiencies are not included. There are also certain minimum values of the area sought for the different device types (above 0.05 cm² for a concentrator cell, 1 cm² for a 1-sun cell, and 800 cm² for a module).

Results are reported for cells and modules made from different semiconductors and for subcategories within each semiconductor

grouping (eg, crystalline, polycrystalline, and thin film). From version 36 onwards, spectral response information is included when available in the form of a plot of the external quantum efficiency (EQE) versus wavelength, either as absolute values or normalised to the peak measured value. Current-voltage (IV) curves have also been included where possible from version 38 onwards. The present version also includes a graphical summary of progress over the past 25 years during which the tables have been published.

Highest confirmed “1-sun” cell and module results are reported in Tables 1–4. Any changes in the tables from those previously published¹ are set in bold type. In most cases, a literature reference is provided that describes either the result reported or a similar result (readers identifying improved references are welcome to submit to the lead author). Table 1 summarises the best-reported measurements for 1-sun (nonconcentrator) single-junction cells and submodules. Table 2 was first introduced in version 49 of these tables and summarises the growing number of cell and submodule results involving high efficiency, 1-sun multiple-junction devices (previously reported in Table 1). Table 3 shows the best results for 1-sun modules. Table 4 contains what might be described as “notable exceptions.” While not conforming to the requirements to be recognised as a class record, the 1-sun cells and modules in this table have notable characteristics that will be of interest to sections

TABLE 1 Confirmed single-junction terrestrial cell and submodule efficiencies measured under the global AM1.5 spectrum (1000 W/m²) at 25°C (IEC 60904-3: 2008, ASTM G-173-03 global)

Classification	Efficiency, %	Area, cm ²	V _{oc} , V	J _{sc} , mA/cm ²	Fill Factor, %	Test Centre (date)	Description
Silicon							
Si (crystalline cell)	26.7 ± 0.5	79.0 (da)	0.738	42.65 ^a	84.9	AIST (3/17)	Kaneka, n-type rear IBC ³
Si (multicrystalline cell)	22.3 ± 0.4 ^b	3.923 (ap)	0.6742	41.08 ^c	80.5	FhG-ISE (8/17)	FhG-ISE, n-type ⁴
Si (thin transfer submodule)	21.2 ± 0.4	239.7 (ap)	0.687 ^d	38.50 ^{d,e}	80.3	NREL (4/14)	Solexel (35 μm thick) ⁵
Si (thin film minimodule)	10.5 ± 0.3	94.0 (ap)	0.492 ^d	29.7 ^{d,f}	72.1	FhG-ISE (8/07)	CSG solar (<2 μm on glass) ⁶
III-V cells							
GaAs (thin film cell)	28.8 ± 0.9	0.9927 (ap)	1.122	29.68 ^g	86.5	NREL (5/12)	Alta Devices ⁷
GaAs (multicrystalline)	18.4 ± 0.5	4.011 (t)	0.994	23.2	79.7	NREL (11/95)	RTI, Ge substrate ⁸
InP (crystalline cell)	24.2 ± 0.5 ^b	1.008 (ap)	0.939	31.15 ^a	82.6	NREL (3/13)	NREL ⁹
Thin film chalcogenide							
CIGS (cell)	21.7 ± 0.5	1.044 (da)	0.718	40.70 ^a	74.3	AIST (1/17)	Solar Frontier ¹⁰
CdTe (cell)	21.0 ± 0.4	1.0623 (ap)	0.8759	30.25 ^e	79.4	Newport (8/14)	First Solar, on glass ¹¹
CZTS (cell)	10.0 ± 0.2	1.113 (da)	0.7083	21.77 ^a	65.1	NREL (3/17)	UNSW ¹²
Amorphous/microcrystalline							
Si (amorphous cell)	10.2 ± 0.3 ^{h,b}	1.001 (da)	0.896	16.36 ^e	69.8	AIST (7/14)	AIST ¹³
Si (microcrystalline cell)	11.9 ± 0.3 ^b	1.044 (da)	0.550	28.72 ^a	75.0	AIST (2/17)	AIST ¹⁴
Perovskite							
Perovskite (cell)	20.9 ± 0.7 ^{i,j}	0.991 (da)	1.125	24.92 ^c	74.5	Newport (7/17)	KRICT ¹⁵
Perovskite (minimodule)	16.0 ± 0.4 ⁱ	16.29 (ap)	0.978 ^d	21.44 ^{d,a}	76.1	Newport (4/17)	Microquanta, 6 serial cells ¹⁶
Dye sensitised							
Dye (cell)	11.9 ± 0.4 ^k	1.005 (da)	0.744	22.47 ^l	71.2	AIST (9/12)	Sharp ¹⁷
Dye (minimodule)	10.7 ± 0.4 ^k	26.55 (da)	0.754 ^d	20.19 ^{d,m}	69.9	AIST (2/15)	Sharp, 7 serial cells ¹⁷
Dye (submodule)	8.8 ± 0.3 ^k	398.8 (da)	0.697 ^d	18.42 ^{d,n}	68.7	AIST (9/12)	Sharp, 26 serial cells ¹⁸
Organic							
Organic (cell)	11.2 ± 0.3 ^o	0.992 (da)	0.780	19.30 ^e	74.2	AIST (10/15)	Toshiba ¹⁹
Organic (minimodule)	9.7 ± 0.3 ^o	26.14 (da)	0.806 ^d	16.47 ^{d,m}	73.2	AIST (2/15)	Toshiba (8 series cells) ²⁰

Abbreviations: (ap), aperture area; (da), designated illumination area; (t), total area; a-Si, amorphous silicon/hydrogen alloy; AIST, Japanese National Institute of Advanced Industrial Science and Technology; CIGS, CuIn_{1-y}Ga_ySe₂; CZTS, Cu₂ZnSnS₄; CZTSS, Cu₂ZnSnS_{4-y}Se_y; FhG-ISE, Fraunhofer Institut für Solare Energiesysteme; nc-Si, nanocrystalline or microcrystalline silicon.

^aSpectral response and current-voltage curve reported in version 50 of these tables.

^bNot measured at an external laboratory.

^cSpectral response and current-voltage curve reported in the present version of these tables.

^dReported on a "per cell" basis.

^eSpectral responses and current-voltage curve reported in version 45 of these tables.

^fRecalibrated from original measurement.

^gSpectral response and current-voltage curve reported in version 40 of these tables.

^hStabilised by 1000 h exposure to 1-sun light at 50°C.

ⁱInitial performance (not stabilised). Reference 21 reviews the stability of similar devices.

^jCertified parameters are average of forward and reverse sweeps performed at 150 mV/s. Efficiency hysteresis of ±0.26% of the certified value was observed at this sweep rate.

^kNot stabilised, initial efficiency. Reference 22 reviews the stability of similar devices.

^lSpectral response and current-voltage curve reported in version 41 of these tables.

^mSpectral response and current-voltage curve reported in version 46 of these tables.

ⁿSpectral response and current-voltage curve reported in version 43 of these tables.

^oInitial performance (not stabilised).

of the photovoltaic community, with entries based on their significance and timeliness.

To encourage discrimination, Table 4 is limited to nominally 12 entries with the present authors having voted for their preferences for inclusion. Readers who have suggestions of results for inclusion into this table are welcome to contact any of the authors with full

details. Suggestions conforming to the guidelines will be included on the voting list for a future issue.

Table 5 shows the best results for concentrator cells and concentrator modules (a smaller number of notable exceptions for concentrator cells and modules additionally is included in Table 5).

TABLE 2 Confirmed multiple-junction terrestrial cell and submodule efficiencies measured under the global AM1.5 spectrum (1000 W/m²) at 25°C (IEC 60904-3: 2008, ASTM G-173-03 global)

Classification	Efficiency, %	Area, cm ²	V _{oc} , V	J _{sc} , mA/cm ²	Fill Factor, %	Test Centre (date)	Description
III-V multijunctions							
5 junction cell (bonded) (2.17/1.68/1.40/1.06/0.73 eV)	38.8 ± 1.2	1.021 (ap)	4.767	9.564	85.2	NREL (7/13)	Spectrolab, 2-terminal ²³
InGaP/GaAs/InGaAs	37.9 ± 1.2	1.047 (ap)	3.065	14.27 ^a	86.7	AIST (2/13)	Sharp, 2-term ²⁴
GaN/P/GaAs (monolithic)	32.8 ± 1.4	1.000 (ap)	2.568	14.56^b	87.7	NREL (9/17)	LG Electronics, 2-term
Multijunctions with c-Si							
GaN/P/GaAs/Si (mech. Stack)	35.9 ± 0.5 ^c	1.002 (da)	2.52/0.681	13.6/11.0	87.5/78.5	NREL (2/17)	NREL/CSEM/EPFL, 4-term ²⁵
GaN/P/GaAs/Si (wafer bonded)	33.3 ± 1.2^c	3.984 (ap)	3.127	12.7^b	83.8	FhG-ISE (8/17)	Fraunhofer ISE, 2-term²⁶
GaN/P/GaAs/Si (monolithic)	19.7 ± 0.7 ^c	3.943 (ap)	2.323	10.0 ^e	84.3	FhG-ISE (8/16)	Fraunhofer ISE
GaN/P/Si (mech. stack)	32.8 ± 0.5 ^c	1.003 (da)	1.09/0.683	28.9/11.1 ^d	85.0/79.2	NREL (12/16)	NREL/CSEM/EPFL, 4-term ²⁵
Perovskite/Si (monolithic)	23.6 ± 0.6 ^f	0.990 (ap)	1.651	18.09 ^e	79.0	NREL (8/16)	Stanford/ASU ²⁷
GaN/P/GaNAs/Ge; Si (spectral split minimodule)	34.5 ± 2.0	27.83 (ap)	2.66/0.65	13.1/9.3	85.6/79.0	NREL (4/16)	UNSW/Azur/Trina, 4-term ²⁸
a-Si/nc-Si multijunctions							
a-Si/nc-Si/nc-Si (thin-film)	14.0 ± 0.4 ^{g,c}	1.045 (da)	1.922	9.94 ^e	73.4	AIST (5/16)	AIST ²⁹
a-Si/nc-Si (thin-film cell)	12.7 ± 0.4 ^{g,c}	1.000(da)	1.342	13.45 ^h	70.2	AIST (10/14)	AIST ^{13,14}

Abbreviations: (ap), aperture area; a-Si, amorphous silicon/hydrogen alloy; (da), designated illumination area; (t), total area; AIST, Japanese National Institute of Advanced Industrial Science and Technology; FhG-ISE, Fraunhofer Institut für Solare Energiesysteme; nc-Si, nanocrystalline or microcrystalline silicon.

^aSpectral response and current-voltage curve reported in version 42 of these tables.

^bSpectral response and current-voltage curve reported in the present version of these tables.

^cNot measured at an external laboratory.

^dSpectral response and current-voltage curve reported in version 50 of these tables.

^eSpectral response and current-voltage curve reported in version 49 of these tables.

^fNot stabilised, initial efficiency. Reference 21 reviews the stability of similar devices.

^gStabilised by 1000 h exposure to 1-sun light at 50°C.

^hSpectral responses and current-voltage curve reported in version 45 of these tables.

TABLE 3 Confirmed terrestrial module efficiencies measured under the global AM1.5 spectrum (1000 W/m²) at a cell temperature of 25°C (IEC 60904-3: 2008, ASTM G-173-03 global)

Classification	Effic. (%)	Area (cm ²)	V _{oc} (V)	I _{sc} (A)	FF (%)	Test Centre (date)	Description
Si (crystalline)	24.4 ± 0.5	13177 (da)	79.5	5.04 ^a	80.1	AIST (9/16)	Kaneka (108 cells) ³
Si (multicrystalline)	19.9 ± 0.4	15143 (ap)	78.87	4.795 ^a	79.5	FhG-ISE (10/16)	Trina solar (120 cells) ³⁰
GaAs (thin film)	25.1 ± 0.8	866.45 (ap)	11.08	2.303^b	85.3	FhG-ISE (11/17)	Alta Devices³¹
CIGS (Cd free)	19.2 ± 0.5	841 (da)	48.0	0.456 ^c	73.7	AIST (1/17)	Solar frontier (70 cells) ³²
CdTe (thin-film)	18.6 ± 0.5	7038.8 (ap)	110.6	1.533 ^d	74.2	NREL (4/15)	First solar, monolithic ³³
CIGS (large)	15.7 ± 0.5	9703 (ap)	28.24	7.254 ^e	72.5	NREL (11/10)	Miasole ³⁴
a-Si/nc-Si (tandem)	12.3 ± 0.3 ^f	14322 (t)	280.1	0.902 ^g	69.9	ESTI (9/14)	TEL solar, Trubbach Labs ³⁵
Organic	8.7 ± 0.3 ^h	802 (da)	17.47	0.569 ⁱ	70.4	AIST (5/14)	Toshiba ²⁰
Multijunction							
InGaP/GaAs/InGaAs	31.2 ± 1.2	968 (da)	23.95	1.506	83.6	AIST (2/16)	Sharp (32 cells) ³⁶

CIGSS = CuInGaSSe; a-Si = amorphous silicon/hydrogen alloy; a-SiGe = amorphous silicon/germanium/hydrogen alloy; nc-Si = nanocrystalline or microcrystalline silicon; Effic. = efficiency; (t) = total area; (ap) = aperture area; (da) = designated illumination area; FF = fill factor

^aSpectral response and current voltage curve reported in version 49 of these tables.

^bSpectral response and current-voltage curve reported in the present version of these tables.

^cSpectral response and current-voltage curve reported in version 50 of these tables.

^dSpectral response and/or current-voltage curve reported in version 47 of these tables.

^eSpectral response reported in version 37 of these tables.

^fStabilised at the manufacturer to the 2% level following IEC procedure of repeated measurements.

^gSpectral response and/or current-voltage curve reported in version 46 of these tables.

^hInitial performance (not stabilised).

ⁱSpectral response and current-voltage curve reported in version 45 of these tables.

TABLE 4 “Notable exceptions”: “Top 10” confirmed cell and module results not class records measured under the global AM1.5 spectrum (1000 W m^{-2}) at 25°C (IEC 60904-3: 2008, ASTM G-173-03 global)

Classification	Efficiency, %	Area, cm^2	V_{oc} , V	J_{sc} , mA/cm^2	Fill Factor, %	Test Centre (date)	Description
Cells (silicon)							
Si (crystalline)	25.0 ± 0.5	4.00 (da)	0.706	42.7^a	82.8	Sandia (3/99) ^b	UNSW p-type PERC top/rear contacts ³⁷
Si (crystalline)	25.8 ± 0.5^c	4.008 (da)	0.7241	42.87^d	83.1	FhG-ISE (7/17)	FhG-ISE, n-type top/rear contacts ³⁸
Si (large)	26.6 ± 0.5	179.74 (da)	0.7403	42.5^e	84.7	FhG-ISE (11/16)	Kaneka, n-type rear IBC ³
Si (multicrystalline)	22.0 ± 0.4	245.83 (t)	0.6717	40.55^d	80.9	FhG-ISE (9/17)	Jinko solar, large p-type ³⁹
GaInP	21.4 ± 0.3	0.2504 (ap)	1.4932	16.31^f	87.7	NREL (9/16)	LG electronics, high bandgap ⁴⁰
GaInAsP/GaInAs	32.6 ± 1.4^c	0.248 (ap)	2.024	19.51^d	82.5	NREL (10/17)	NREL, monolithic tandem
Cells (chalcogenide)							
CIGS (thin-film)	22.6 ± 0.5	0.4092 (da)	0.7411	37.76^f	80.6	FhG-ISE (2/16)	ZSW on glass ⁴¹
CIGSS (cd free)	22.0 ± 0.5	0.512 (da)	0.7170	39.45^f	77.9	FhG-ISE (2/16)	Solar frontier on glass ¹⁰
CdTe (thin-film)	22.1 ± 0.5	0.4798 (da)	0.8872	31.69^g	78.5	Newport (11/15)	First solar on glass ⁴²
CZTSS (thin-film)	12.6 ± 0.3	0.4209 (ap)	0.5134	35.21^h	69.8	Newport (7/13)	IBM solution grown ⁴³
CZTS (thin-film)	11.0 ± 0.2	0.2339(da)	0.7306	21.74^e	69.3	NREL (3/17)	UNSW on glass ¹²
Cells (other)							
Perovskite (thin-film)	22.7 ± 0.8^i	0.0935 (ap)	1.144	24.92^d	79.6	Newport (7/17)	KRICT ¹⁵
Organic (thin-film)	12.1 ± 0.3^k	0.0407 (ap)	0.8150	20.27^e	73.5	Newport (2/17)	Phillips 66

Abbreviations: (ap), aperture area; (da), designated illumination area; (t), total area; AIST, Japanese National Institute of Advanced Industrial Science and Technology; CIGSS = CuInGaSe ; CZTS = $\text{Cu}_2\text{ZnSnS}_4$; CZTSS = $\text{Cu}_2\text{ZnSnS}_{4-y}\text{Se}_y$; FhG-ISE, Fraunhofer-Institut für Solare Energiesysteme; NREL, National Renewable Energy Laboratory.

^aSpectral response reported in version 36 of these tables.

^bRecalibrated from original measurement.

^cNot measured at an external laboratory.

^dSpectral response and current-voltage curves reported in the present version of these tables.

^eSpectral response and current-voltage curves reported in version 50 of these tables.

^fSpectral response and current-voltage curves reported in version 49 of these tables.

^gSpectral response and/or current-voltage curves reported in version 46 of these tables.

^hSpectral response and current-voltage curves reported in version 44 of these tables.

ⁱStability not investigated. Reference 21 documents stability of similar devices. Certified parameters are average of forward and reverse sweeps performed at 150 mV/s . Efficiency hysteresis of $\pm 0.51\%$ of the certified value was observed at this sweep rate.

^jSpectral response and current-voltage curves reported in version 48 of these tables.

^kStability not investigated.

2 | NEW RESULTS

Ten new results are reported in the present version of these tables. The first new result in Table 1 is a new efficiency record for a multicrystalline silicon (mc-Si) cell. An efficiency of 22.3% is reported for a 4-cm^2 cell using an n-type mc-Si wafer as substrate, fabricated by Fraunhofer Institute for Solar Energy Systems (FhG-ISE), and measured at the same institution.⁴

A second new result in Table 1 documents achievement of the landmark efficiency of 20% for a 1-cm^2 lead halide perovskite solar cell. An efficiency of 20.9% was measured for a 1.0-cm^2 perovskite cell fabricated by the Korean Research Institute of Chemical Technology¹⁵ and measured at the Newport PV Laboratory. These perovskite results represent initial efficiencies, with the long-term stability of these devices not investigated.

Two new results are reported in Table 2 for 1-sun, multijunction devices. An efficiency of 32.8% was measured for a 1-cm^2 GaInP/GaAs monolithic 2-junction, 2-terminal device fabricated by LG Electronics and measured at the US National Renewable Energy Laboratory (NREL). Efficiency for a 2-terminal, triple-junction GaInP/GaInAs cell wafer-bonded to a Si cell was increased to 33.3% for a cell fabricated and measured at FhG-ISE.

One new module result is reported in Table 3. An efficiency of 25.1% is reported for a 866-cm^2 GaAs module fabricated by Alta Devices and measured at FhG-ISE.

Four new cell results are reported as notable exceptions in Table 4. An efficiency of 25.8% has been confirmed for a 4-cm^2 n-type crystalline silicon cell with contacts on both top and rear surfaces, fabricated and measured at FhG-ISE,³⁸ a record for a cell with this traditional type of contacting. An efficiency of 22.0% has

TABLE 5 Terrestrial concentrator cell and module efficiencies measured under the ASTM G-173-03 direct beam AM1.5 spectrum at a cell temperature of 25°C

Classification	Effic., %	Area, cm ²	Intensity ^a , suns	Test Centre (date)	Description
Single cells					
GaAs	29.3 ± 0.7 ^b	0.09359 (da)	49.9	NREL (10/16)	LG Electronics
Si	27.6 ± 1.2 ^c	1.00 (da)	92	FhG-ISE (11/04)	Amonix back-contact ⁴⁴
CIGS (thin film)	23.3 ± 1.2 ^{d,e}	0.09902 (ap)	15	NREL (3/14)	NREL ⁴⁵
Multijunction cells					
GalnP/GaAs; GalnAsP/GalnAs	46.0 ± 2.2 ^f	0.0520 (da)	508	AIST (10/14)	Soitec/CEA/FhG-ISE 4j bonded ⁴⁶
GalnP/GaAs/GalnAs/GalnAs	45.7 ± 2.3 ^{d,g}	0.09709 (da)	234	NREL (9/14)	NREL, 4j monolithic ⁴⁷
InGaP/GaAs/InGaAs	44.4 ± 2.6 ^h	0.1652 (da)	302	FhG-ISE (4/13)	Sharp, 3j inverted metamorphic ⁴⁸
GalnAsP/GalnAs	35.5 ± 1.2^{i,d}	0.10031 (da)	38	NREL (10/17)	NREL 2-junction (2j)
Minimodule					
GalnP/GaAs; GalnAsP/GalnAs	43.4 ± 2.4 ^{d,j}	18.2 (ap)	340 ^k	FhG-ISE (7/15)	Fraunhofer ISE 4j (lens/cell) ⁴⁹
Submodule					
GalnP/GalnAs/Ge; Si	40.6 ± 2.0 ^j	287 (ap)	365	NREL (4/16)	UNSW 4j split spectrum ⁵⁰
Modules					
Si	20.5 ± 0.8 ^d	1875 (ap)	79	Sandia (4/89) ^l	Sandia/UNSW/ENTECH (12 cells) ⁵¹
Three junction (3j)	35.9 ± 1.8 ^m	1092 (ap)	N/A	NREL (8/13)	Amonix ⁵²
Four junction (4j)	38.9 ± 2.5 ⁿ	812.3 (ap)	333	FhG-ISE (4/15)	Soitec ⁵³
"Notable exceptions"					
Si (large area)	21.7 ± 0.7	20.0 (da)	11	Sandia (9/90) ^k	UNSW laser grooved ⁵⁴
Luminescent minimodule	7.1 ± 0.2	25(ap)	2.5 ^k	ESTI (9/08)	ECN Petten, GaAs cells ⁵⁵

Abbreviations: (ap), aperture area; (da), designated illumination area; CIGS, CuInGaSe₂; Effic., efficiency; FhG-ISE, Fraunhofer-Institut für Solare Energiesysteme; NREL, National Renewable Energy Laboratory.

^aOne sun corresponds to direct irradiance of 1000 Wm⁻².

^bSpectral response and current-voltage curve reported in version 50 of these tables.

^cMeasured under a low aerosol optical depth spectrum similar to ASTM G-173-03 direct.⁵⁶

^dNot measured at an external laboratory.

^eSpectral response and current-voltage curve reported in version 44 of these tables.

^fSpectral response and current-voltage curve reported in version 45 of these tables.

^gSpectral response and current-voltage curve reported in version 46 of these tables.

^hSpectral response and current-voltage curve reported in version 42 of these tables.

ⁱSpectral response and current-voltage curve reported in the present version of these tables.

^jDetermined at IEC 62670-1 CSTC reference conditions.

^kGeometric concentration.

^lRecalibrated from original measurement.

^mReferenced to 1000 W/m² direct irradiance and 25°C cell temperature using the prevailing solar spectrum and an in-house procedure for temperature translation.

ⁿMeasured under IEC 62670-1 reference conditions following the current IEC power rating draft 62670-3.

also been confirmed for a large area 246-cm² p-type multicrystalline cell fabricated by Jinko Solar using Passivated Emitter and Rear Cell technology,³⁹ with the cell also measured at FhG-ISE.

A third new result in Table 4 is 32.6% efficiency for a small area (0.25 cm²) GalnAsP/GalnAs monolithic, 2-junction, 2-terminal, 1-sun cell fabricated by and measured at NREL.⁵⁷ An efficiency of 22.7% has also been measured for a small area (0.09 cm²) lead halide perovskite cell fabricated by Korean Research Institute of Chemical Technology and measured at Newport.¹⁵ For the previous 2 cells, cell area is too small for classification as an outright record. Solar cell efficiency targets in governmental research programs generally have

been specified in terms of a cell area of 1 cm² or larger.⁵⁸⁻⁶⁰ Additionally, the certificate for the perovskite cell advises that the results "apply at the time of the test and do not imply future performance."

The final new result in Table 5 is improvement in the efficiency of a small area, 2-junction, 2-terminal tandem GalnAsP/GalnAs concentrator cell to 35.5% under 38-suns concentration (direct irradiance of 38 kW/m²). The cell was fabricated by and measured at NREL.

The EQE spectra for the new silicon cell results reported in the present issue of these tables are shown in Figure 1A, with Figure 1B showing the current density-voltage (JV) curves for the

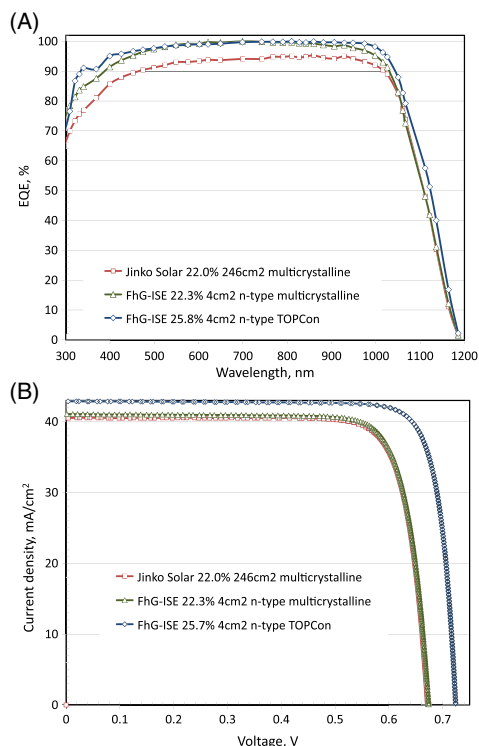


FIGURE 1 A, Normalised external quantum efficiency (EQE) for the new silicon cell results reported in this issue (some results normalised). B, Corresponding current density-voltage curves for the same devices. FhG-ISE, Fraunhofer Institute for Solar Energy Systems [Colour figure can be viewed at wileyonlinelibrary.com]

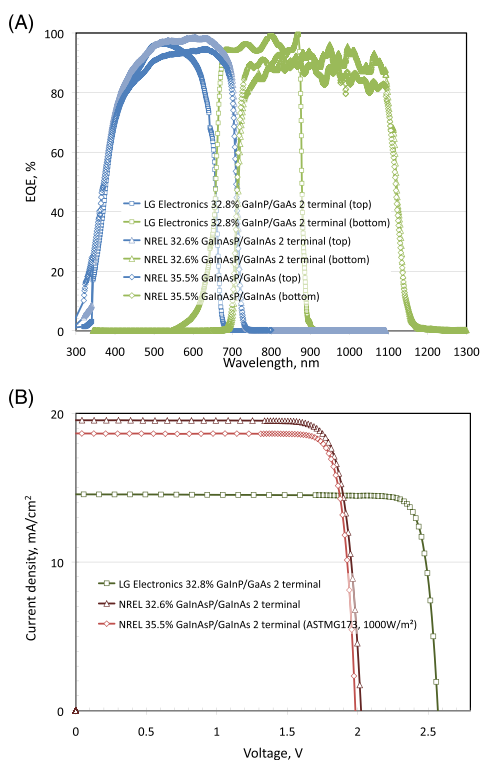


FIGURE 2 A, External quantum efficiency (EQE) for the new 2-junction multijunction cell results reported in this issue (some results normalised). B, Corresponding current density-voltage curves. NREL, National Renewable Energy Laboratory [Colour figure can be viewed at wileyonlinelibrary.com]

same devices. Figure 2A shows the EQE for the new 2-junction multijunction cell results with Figure 2B showing their current JV curves. Figure 3A,B shows the corresponding EQE and JV curves for the new perovskite and GaAs cell results.

3 | PROGRESS OVER THE LAST 25 YEARS

Figure 4 reports 25 years of progress in confirmed cell and module efficiencies since the first version of these tables was published in 1993. Figure 4A shows progress with 1-sun cells of $\geq 1\text{-cm}^2$ area. Recent progress with perovskite and CdTe cells has been most notable, with good progress also with CIGS and both crystalline and mc-Si. Figure 4B shows similar progress with photovoltaic modules with CdTe, CIGS, and the mainstream mc-Si being the recent standouts. Figure 4C shows the results for concentrator cells and modules. Impressive progress has been made with monolithic III-V MJ cells where efficiency has been improved from 31.8% to 46.0% over the 25-year period (efficiency in this case is boosted relative to results in Figure 4A,B since based on only the direct normal component of the solar spectrum, with the diffuse component neglected in the efficiency calculation).

DISCLAIMER

While the information provided in the tables is provided in good faith, the authors, editors, and publishers cannot accept direct responsibility for any errors or omissions.

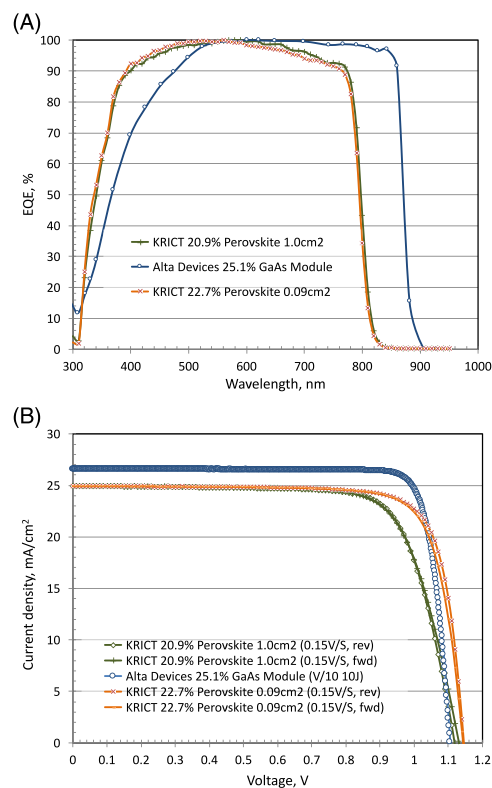


FIGURE 3 A, External quantum efficiency (EQE) for the new perovskite and GaAs cell results reported in this issue (all results normalised). B, Corresponding current density-voltage curves. KRICT, Korean Research Institute of Chemical Technology [Colour figure can be viewed at wileyonlinelibrary.com]

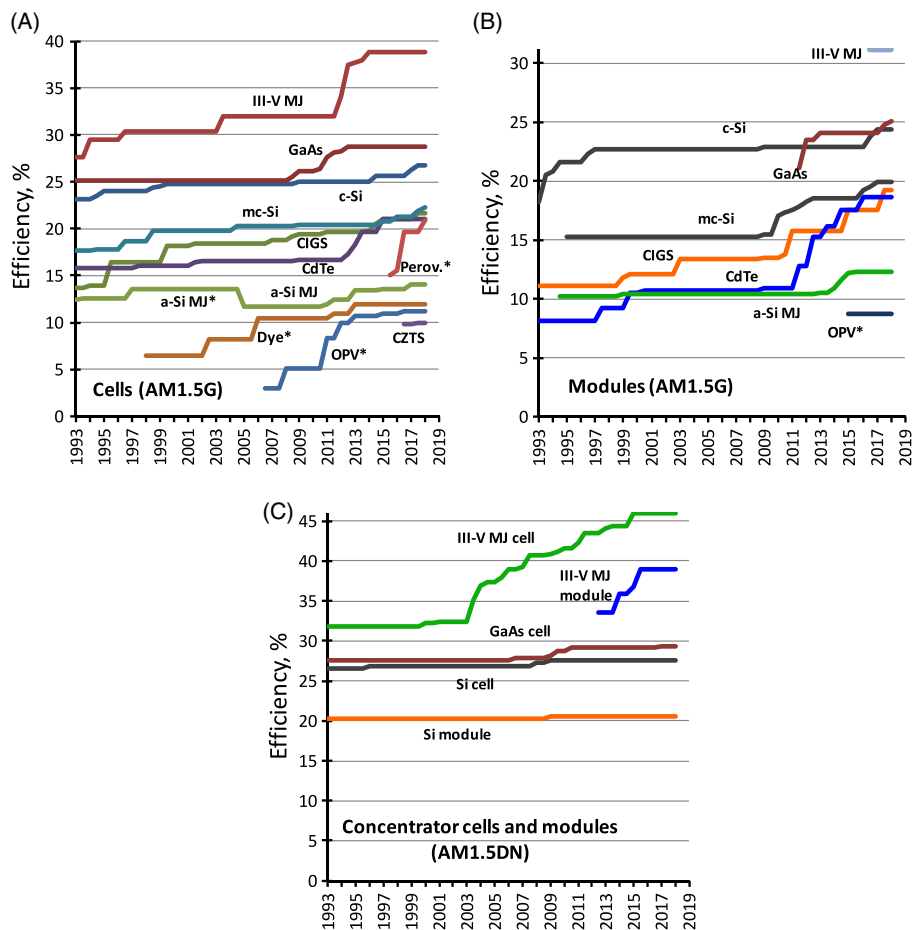


FIGURE 4 Twenty-five years of progress: A, highest confirmed efficiencies for $\geq 1\text{-cm}^2$ area cells fabricated using the different technologies shown (*the results for the OPV, dye-sensitised and perovskite cells are unstabilised results as are those for a-Si multijunction cells prior to 2005). B, highest confirmed module results for modules sizes $\geq 800\text{-cm}^2$. C, highest confirmed concentrator cell and module results [Colour figure can be viewed at wileyonlinelibrary.com]

ACKNOWLEDGEMENT

The Australian Centre for Advanced Photovoltaics commenced operation in February 2013 with support from the Australian Government through the Australian Renewable Energy Agency (ARENA). The Australian Government does not accept responsibility for the views, information, or advice expressed herein. The work by D. Levi was supported by the U.S. Department of Energy under Contract No. DE-AC36-08-GO28308 with the National Renewable Energy Laboratory. The work at AIST was supported in part by the Japanese New Energy and Industrial Technology Development Organisation (NEDO) under the Ministry of Economy, Trade and Industry (METI).

ORCID

Martin A. Green <http://orcid.org/0000-0002-8860-396X>

Yoshihiro Hishikawa <http://orcid.org/0000-0002-8420-9260>

Anita W.Y. Ho-Baillie <http://orcid.org/0000-0001-9849-4755>

REFERENCES

- Green MA, Emery K, Hishikawa Y, et al. Solar cell efficiency tables (version 50). *Prog Photovolt Res Appl*. 2017;25(7):668-676.
- Green MA, Emery K, Hishikawa Y, Warta W. Solar cell efficiency tables (version 33). *Prog Photovolt Res Appl*. 2009;17(1):85-94.
- Yoshikawa K, Kawasaki H, Yoshida W, et al. Silicon heterojunction solar cell with interdigitated back contacts for a photoconversion efficiency over 26%. *Nat Energy*. 2017;2(5):17032
- Benick J, Richter A, Müller R, et al. High-efficiency n-type HP mc silicon solar cells. *IEEE J Photovoltaics*. 2017;7(5):1171-1175.
- Moslehi MM, Kapur P, Kramer J, Rana V, Seutter S, Deshpande A, Stalcup T, Kommera S, Ashjaee J, Calcaterra A, Grupp D, Dutton D, Brown R. World-record 20.6% efficiency 156 mm x 156 mm full-square solar cells using low-cost kerfless ultrathin epitaxial silicon & porous silicon lift-off technology for industry-leading high-performance smart PV modules. *PV Asia Pacific Conference (APVIA/PVAP)*, 24 October 2012.
- Keevers MJ, Young TL, Schubert U, Green MA. 10% efficient CSG minimodules. *22nd European Photovoltaic Solar Energy Conference*, Milan, 2007.
- Kayes BM, Nie H, Twist R, Spruytte SG, Reinhardt F, Kizilyalli IC, Hignashi GS. 27.6% conversion efficiency, a new record for single-junction solar cells under 1 sun illumination. *Proceedings of the 37th IEEE Photovoltaic Specialists Conference*, 2011.
- Venkatasubramanian R, O'Quinn BC, Hills JS, Sharps PR, Timmons ML, Hutchby JA, Field H, Ahrenkiel A, Keyes B. 18.2% (AM1.5) efficient GaAs solar cell on optical-grade polycrystalline Ge substrate. *Conference Record, 25th IEEE Photovoltaic Specialists Conference*, Washington, May 1997, 31-36.
- Wanlass M. Systems and methods for advanced ultra-high-performance InP solar cells. US Patent 9,590,131 B2, 7 March 2017.

10. Kato T, Handa A, Yagioka T, Matsuura T, Yamamoto K, Higashi S, Wu J-L, Tai KF, Hiroi H, Yoshiyama T, Sakai T, Sugimoto H. Enhanced efficiency of Cd-free Cu(In,Ga)(Se,S)₂ minimodule via (Zn,Mg)O second buffer layer and alkali post treatment. *44th IEEE Photovoltaic Specialists Conference*, Washington DC, 25–30 June 2017.
11. First Solar press release, first solar builds the highest efficiency thin film PV cell on record, 5 August 2014.
12. Sun K, Yan C, Liu F, et al. Beyond 9% efficient kesterite Cu₂ZnSnS₄ solar cell: fabricated by using Zn_{1-x}CdxS buffer layer. *Adv Energy Mater.* 2016;6: 1600046 (DOI:<https://doi.org/10.1002/aenm.201600046>):12).
13. Matsui T, Sai H, Suezaki T, Matsumoto M, Saito K, Yoshida I, Kondo M. Development of highly stable and efficient amorphous silicon based solar cells. *Proc. 28th European Photovoltaic Solar Energy Conference 2013*; 2213–2217.
14. Sai H, Maejima K, Matsui T, et al. High-efficiency microcrystalline silicon solar cells on honeycomb textured substrates grown with high-rate VHF plasma-enhanced chemical vapor deposition. *Jpn J Appl Phys.* 2015;54(8S1): 08KB05:08KB05
15. Yang WS, Noh JH, Jeon NJ, et al. High-performance photovoltaic perovskite layers fabricated through intramolecular exchange. *Science.* 2015;348(6240):1234–1237.
16. <http://microquanta.com/newsitem/277743967> (dated 17 March 2017).
17. Komiya R, Fukui A, Murofushi N, Koide N, Yamanaka R and Katayama H. Improvement of the conversion efficiency of a monolithic type dye-sensitized solar cell module. *Technical Digest, 21st International Photovoltaic Science and Engineering Conference*, Fukuoka, November 2011; 2C-50-08.
18. Kawai M. High-durability dye improves efficiency of dye-sensitized solar cells. *Nikkei Electronics* 2013; Feb.1 (http://techon.nikkeibp.co.jp/english/NEWS_EN/20130131/263532/) (accessed 23 October, 2013)
19. Mori S, Oh-oka H, Nakao H, Gotanda T, Nakano Y, Jung H, Iida A, Hayase R, Shida N, Saito M, Todoriki K, Asakura T, Matsui A, Hosoya M. Organic photovoltaic module development with inverted device structure. *MRS Proceedings, Vol. 1737*, 2015 (DOI: <https://doi.org/10.1557/opl.2015.540>).
20. Hosoya M, Oooka H, Nakao H, Gotanda T, Mori S, Shida N, Hayase R, Nakano Y, Saito M. Organic thin film photovoltaic modules. *Proceedings of the 93rd Annual Meeting of the Chemical Society of Japan* 2013; 21–37.
21. Han Y, Meyer S, Dkhissi Y, et al. Degradation observations of encapsulated planar CH₃NH₃PbI₃ perovskite solar cells at high temperatures and humidity. *J Mater Chem A.* 2015;3(15):8139–8147.
22. Krašovec UO, Bokalič M, Topič M. Ageing of DSSC studied by electroluminescence and transmission imaging. *Sol Energy Mater Sol Cells.* 2013;117:67–72.
23. Chiu PT, Law DL, Woo RL, Singer S, Bhusari D, Hong WD, Zakaria A, Boisvert JC, Mesropian S, King RR, Karam NH. 35.8% space and 38.8% terrestrial 5J direct bonded cells. *Proc. 40th IEEE Photovoltaic Specialist Conference*, Denver, June 2014; 11–13.
24. Sasaki K, Agui T, Nakaido K, Takahashi N, Onitsuka R, Takamoto T. *Proceedings, 9th International Conference on Concentrating Photovoltaics Systems*. Japan: Miyazaki; 2013.
25. Essig S, Allebé C, Remo T, et al. Raising the one-sun conversion efficiency of III–V/Si solar cells to 32.8% for two junctions and 35.9% for three junctions. *Nature Energy.* 2017;2(9):17144. <https://doi.org/10.1038/nenergy.2017.144>
26. https://www.ise.fraunhofer.de/content/dam/ise/en/documents/News/2017/0917_News_31_Percent_for-Silicon-based-multi-junction-solar-cell_e.pdf (dated 24 March 2017).
27. Bush KA, Palmstrom AF, Yu ZJ, et al. 23.6%-efficient monolithic perovskite/silicon tandem solar cells with improved stability. *Nature Energy.* 2017;2(4):17009
28. Green MA, Keevers MJ, Concha Ramon B, Jiang Y, Thomas I, Lasich JB, Verlinden, PJ, Yang Y, Zhang X, Emery K, Moriarty T, King RR, Bensch W. Improvements in sunlight to electricity conversion efficiency: above 40% for direct sunlight and over 30% for global. Paper 1AP.1.2, *European Photovoltaic Solar Energy Conference 2015*, Hamburg, September 2015.
29. Sai H, Matsui T, Koida T, et al. Triple-junction thin-film silicon solar cell fabricated on periodically textured substrate with a stabilized efficiency of 13.6%. *Appl Phys Lett.* 2015;106(21):213902. <https://doi.org/10.1063/1.4921794>
30. Verlinden PJ. *Will we have > 22% efficient multi-crystalline silicon solar cells?* PVSEC 26, Singapore, 24–28 October, 2016.
31. Mattos LS, Scully SR, Syfu M, Olson E, Yang L, Ling C, Kayes BM, He G. New module efficiency record: 23.5% under 1-sun illumination using thin-film single-junction GaAs solar cells. *Proceedings of the 38th IEEE Photovoltaic Specialists Conference*, 2012.
32. Sugimoto H. High efficiency and large volume production of CIS-based modules. *40th IEEE Photovoltaic Specialists Conference*, Denver, June 2014.
33. First Solar press release. First Solar achieves world record 18.6% thin film module conversion efficiency, 15 June 2015.
34. <http://www.miasole.com> (accessed 22 May, 2015).
35. Cashmore JS, Apolloni M, Braga A, et al. Improved conversion efficiencies of thin-film silicon tandem (MICROMORPH™) photovoltaic modules. *Sol Energy Mater Sol Cells.* 2016;144:84–95. <https://doi.org/10.1016/j.solmat.2015.08.022>
36. Takamoto T. Application of InGaP/GaAs/InGaAs triple junction solar cells to space use and concentrator photovoltaic. *40th IEEE Photovoltaic Specialists Conference*, Denver, June 2014.
37. Zhao J, Wang A, Green MA, Ferrazza F. Novel 19.8% efficient "honeycomb" textured multicrystalline and 24.4% monocrystalline silicon solar cells. *Appl Phys Lett.* 1998;73(14):1991–1993.
38. Richter A, Benick J, Feldmann F, Fell A, Hermle M, Glunz SW. n-Type Si solar cells with passivating electron contact: identifying sources for efficiency limitations by wafer thickness and resistivity variation. *Sol Energy Mater Sol Cells.* 2017;173:96–105.
39. https://www.jinkosolar.com/press_detail_1380.htm (accessed 4 May 2017).
40. Kim S, Hwang ST, Yoon W, Lee HM. High performance GaAs solar cell using heterojunction emitter and its further improvement by ELO technique. Paper 4CV.1.27, *European Photovoltaic Solar Energy Conference 2016*, Munich, June 2016.
41. https://www.zsw-bw.de/fileadmin/user_upload/PDFs/Pressemitteilungen/2016/pr09-2016-ZSW-WorldRecordCIGS.pdf (dated 15 June 2016, accessed 25 October 2016).
42. First Solar press release. First Solar achieves yet another cell conversion efficiency world record, 24 February 2016.
43. Wang W, Winkler MT, Gunawan O, et al. Device characteristics of CZTSSe thin-film solar cells with 12.6% efficiency. *Adv Energy Mater.* 2013;4(7). <https://doi.org/10.1002/aenm.201301465>
44. Slade A, Garboushian V. 27.6% efficient silicon concentrator cell for mass production. *Technical Digest, 15th International Photovoltaic Science and Engineering Conference*, Shanghai, October 2005; 701.
45. Ward JS, Ramanathan K, Hasoon FS, et al. A 21.5% efficient Cu(In,Ga)Se₂ thin-film concentrator solar cell. *Prog Photovolt Res Appl.* 2002;10(1):41–46.
46. Press release, Fraunhofer Institute for Solar Energy Systems, 1 December 2014 (accessed at <http://www.ise.fraunhofer.de/en/press-and-media/press-releases/press-releases-2014/new-world-record-for-solar-cell-efficiency-at-46-percent> on 7 December 2014).
47. NREL Press release NR-4514, 16 December 2014.
48. Press release, Sharp Corporation, 31 May 2012 (accessed at <http://sharp-world.com/corporate/news/120531.html> on 5 June 2013).
49. Steiner M, Siefert G, Schmidt T, Wiesenfarth M, Dimroth F, Bett AW. 43% sun light to electricity conversion efficiency using CPV. *IEEE Journal of Photovoltaics.* 2016;6(4):1020–1024.

50. Green MA, Keevers MJ, Thomas I, Lasich JB, Emery K, King RR. 40% efficient sunlight to electricity conversion. *Prog Photovolt Res Appl*. 2015;23(6):685-691.
51. Chiang CJ and Richards EH. A 20% efficient photovoltaic concentrator module. *Conf. Record, 21st IEEE Photovoltaic Specialists Conference*, Kissimmee, May 1990: 861-863.
52. <http://amonix.com/pressreleases/amonix-achieves-world-record-359-module-efficiency-rating-nrel-4> (accessed 23 October 2013).
53. van Riesen S, Neubauer M, Boos A, Rico MM, Gourdel C, Wanka S, Krause R, Guernard P, Gombert A. New module design with 4-junction solar cells for high efficiencies. *Proceedings of the 11th Conference on Concentrator Photovoltaic Systems*, 2015.
54. Zhang F, Wenham SR, Green MA. Large area, concentrator buried contact solar cells. *IEEE Trans Electron Dev*. 1995;42(1):144-149.
55. Slooff LH, Bende EE, Burgers AR, et al. A luminescent solar concentrator with 7.1% power conversion efficiency. *Phys Stat Sol (RRL)*. 2008;2(6):257-259.
56. Gueymard CA, Myers D, Emery K. Proposed reference irradiance spectra for solar energy systems testing. *Sol Energy*. 2002;73(6):443-467.
57. <https://www.nrel.gov/news/program/2017/team-demonstrates-record-efficiency-dual-junction-solar-cell.html> (accessed 4 May 2017).
58. Program milestones and decision points for single junction thin films. *Annual Progress Report 1984, Photovoltaics, Solar Energy Research Institute, Report DOE/CE-0128*, June 1985; 7.
59. Sakata I, Tanaka Y, Koizawa K. Japan's new national R&D program for photovoltaics. *Photovoltaic Energy Conversion, Conference Record of the 2006 IEEE 4th World Conference*, Vol. 1, May 2008; 1-4.
60. Jäger-Waldau, A (Ed.). *PVNET: European roadmap for PV R&D*, EUR 21087 EN, 2004.

How to cite this article: Green MA, Hishikawa Y, Dunlop ED, Levi DH, Hohl-Ebinger J, Ho-Baillie AWY. Solar cell efficiency tables (version 51). *Prog Photovolt Res Appl*. 2018;26:3-12. <https://doi.org/10.1002/ppp.2978>

APPENDIX A

LIST OF DESIGNATED TEST CENTRES

A list of designated test centres follows. Results from additional ISO/IEC17025 certified centres participating in international round robins involving cells of a similar type to those being reported will also be considered on a case-by-case basis.

European Solar Test Installation (ESTI),
CEC Joint Research Centre,
Via E. Fermi 2749, 21020 Ispra (Varese), Italy.
Contact: Dr Ewan Dunlop
Telephone: +39 332-789090
Facsimile: +39 332-789-268
Email: esti.services@jrc.ec.europa.eu
(cells and modules)

Fraunhofer-Institut für Solare Energiesysteme ISE,
Heidenhofstraße 2, D-79110 Freiburg, Germany.
Contact (CalLab PV Cells): Dr Jochen Hohl-Ebinger
Phone: +49 (0) 761 4588-5359
Facsimile: +49 (0) 761 4588-9359
Email: jochen.hohl-ebinger@ise.fraunhofer.de

Contact (CalLab PV Modules): Frank Neuberger,
Phone: +49 (0) 761 4588-5280
Facsimile: +49 (0) 761 4588-9280
Email: frank.neuberger@ise.fraunhofer.de
(terrestrial, space, and concentrator cells and modules)

Institut für Solarenergieforschung GmbH (ISFH),
Calibration and Test Center (CalTeC), Solar Cells Laboratory
Am Ohrberg 1, D-31860 Emmerthal, Germany.
Contact: Dr Karsten Bothe
Phone: +49 (0) 5151 999 425
Facsimile: +49 (0) 5151 999 400
Mobile: +49 (0) 176 151 999 02
Email: k.bothe@isfh.de
(terrestrial cells)

Japan Electrical Safety & Environment Technology Laboratories (JET),
1-12-28 Motomiya Tsurumi-ku, Yokohama-shi, Kanagawa,
230-004 Japan.
Contact: Hiromi Tobita
Phone: +81-45-570-2073
Email: tobita@jet.or.jp
(terrestrial cells and modules)

National Institute of Advanced Industrial Science and Technology (AIST),
Central 2, Umezono 1-1-1, Tsukuba, Ibaraki, 305-8568 Japan.
Contact: Dr Yoshihiro Hishikawa
Telephone: +81 29-861-5780
Facsimile: +81 29-861-5829
Email: y-hishikawa@aist.go.jp
(terrestrial and concentrator cells and modules)

National Renewable Energy Laboratory (NREL),
15013 Denver West Parkway, Golden, CO 80401, USA.
Contact: Dean Levi
Telephone: +1 303-384-6632
Facsimile: +1 303-384-6604
Email: dean.levi@nrel.gov
(terrestrial, space, and concentrator cells and modules)

Newport PV Lab,
31950 Frontage Road, Bozeman, MT 59715, USA.
Contact: Geoffrey Wicks
Lab: +1 406-556-2469 Office: +1 406-556-2489
Email: geoffrey.wicks@newport.com
(terrestrial cells)

APPENDIX B

AREA DEFINITIONS

The area of the cell or module is a key parameter in determining efficiency. The areas used in the tables conform to 1 of the 3 following classifications illustrated in Figure 5:

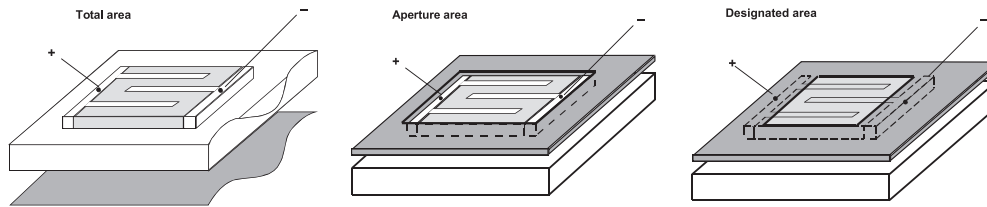


FIGURE 5 Area classifications: total area (shown grey), aperture area, and designated illumination area (the latter 2 areas are the areas not covered by the mask; masking is not required if the test centre is satisfied that there is no response from the areas shown masked)

1. Total area: The total projected area of the cell or module. This is the preferred area for reporting of results. For the case of a cell attached to glass, the total area would be the area of the glass sheet. For a module, it would include the area of frames.
2. Aperture area: The portion of the total cell or module area that includes all essential components, including active material, busbars, fingers, and interconnects. In principle, during testing, illumination is restricted to this portion such as by masking. Such restriction is not essential if the test centre is satisfied that there is no response from light incident outside the assigned aperture area.
3. Designated illumination area: A portion of the cell or module area from which some cell or module contacting components are excluded. In principle, during testing, illumination is restricted to this portion such as by masking. Such restriction is not essential if the test centre is satisfied that there is no response from light incident outside the assigned designated illumination area. For concentrator cells, cell busbars would lie outside of the area designed for illumination and this area classification would be the most appropriate. For a cell on insulating substrates, cell contacts may lie outside the designated illumination area. For modules, cell string interconnects may lie outside the masked area.